Table S1. Crystallographic data and structural refinement for **Gd-MOF**

Compound	Gd-MOF
Chemical Formula	$C_{25}H_{21}GdN_6O_{10}$
Formula Weight (g/mol)	722.73
Temperature (K)	113.15
Wavelength (Å)	0.71073
Crystal System	Tetragonal
Space Group	$P4_14_12$
a (Å)	8.9056(13)
b (Å)	8.9056(13)
c (Å)	33.485(7)
α (°)	90
β (°)	90
γ (°)	90
Z	4
V (Å^3)	2655.7(9)
Density (g/cm^3)	1.808
μ (mm^{-1})	2.567
F (000)	1428
Theta (°) Range for Data Coll.	2.2870 to 27.8944
Reflections Collected	22667
Independent Reflections	3153
Reflections with $I>2\sigma(I)$	2921
R_{int}	0.0593
No. of Parameters refined	200
GOF on F^2	1.138
Final R_1/wR_2 ($I>2\sigma(I)$)	0.0410/0.1150
R_1/wR_2 (all data)	0.0435/0.1172
Largest diff. peak and hole (eÅ^{-3})	0.730/-1.531

Table S2. Selected bond lengths (Å) for **Gd-MOF**.

Bond	Length/ Å	Bond	Length/ Å
Gd1-O1	2.417(6)	O3-C8	1.264(9)
Gd1-O1^1	2.417(6)	O4-C8	1.267(9)
Gd1-O2^1	2.482(6)	O5-C13	1.270(12)
Gd1-O2	2.482(6)	O6-C13	1.319(13)
Gd1-O3^2	2.447(5)	N1-C5	1.399(10)
Gd1-O3^3	2.447(5)	N1-C9	1.427(11)
Gd1-O4^2	2.517(6)	N2-C10	1.395(12)

Gd1-O4[3]	2.517(6)	N2-C12	1.298(13)
Gd1-O5	2.376(9)	N3-C11	1.358(14)
O1-C7	1.273(10)	N3-C12	1.357(14)
O2-C7	1.277(10)		

Symmetry codes: [1]1+Y,-1+X,1-Z; [2]1/2+X,-1/2-Y,3/4-Z; [3]1/2-Y,-1/2+X,1/4+Z

Table S3 Reports for the proton conductivity properties of some UiO-66 derivatives.

Species	σ (S cm^{-1})	T (°C) and RH%	Reference
Zr-MOF	1.81×10^{-2}	353 K and 98% RH	This work
UiO-66(SO_3H)$_2$	8.4×10^{-2}	80°C and 90% relative humidity,	S1
imidazole@UiO-67	1.44×10^{-3}	120 °C under anhydrous conditions	S2
DT-UiO-66	4.47×10^{-3}	373 K and 100% relative humidity (RH)	S3
60-UiO-66-1.8	3×10^{-2}	100°C and under 98% relative humidity	S4
PSM 1	1.64×10^{-1}	80 °C	S5
PSM 2	4.66×10^{-3}	80 °C	S5
UiO-66-SO_3H	0.34×10^{-2}	303 K and ~97% relative humidity	S6
UiO-66-2COOH	0.10×10^{-2}	303 K and ~97% relative humidity	S6

References

S1. W. J. Phang, H. Jo, W. R. Lee, J. H. Song, K. Yoo, B. Kim and C. S. Hong, *Angew. Chem. Int. Ed.*, 2015, **54**, 5142 –5146.

S2. S. Liu, Z. Yue and Y, Liu, *Dalton Trans*., 2015, **44**, 12976–12980.

S3. L. Feng, J. Lan, F. Chen, H. Hou and H. Zhou, *Dalton Trans*., 2021, **50**, 5943–5950.

S4. Q.-Q. Liu, S.-S. Liu, X.-F. Liu, X.-J. Xu, X.-Y. Dong, H.-J. Zhang and S.-Q. Zang, *Inorg. Chem*., 2022, **61**, 3406-3411.

S5. S. Mukhopadhyay, J. Debgupta, C. Singh, R. Sarkar, O. Basu and S. K. Das, *ACS Appl. Mater. Interfaces* 2019, **11**, 13423-13432.

S6. F. Yang, H. Huang, X. Wang, F. Li, Y. Gong, C. Zhong and J.-R. Li, *Cryst. Growth Des.*, 2015, **15**, 5827-5833.

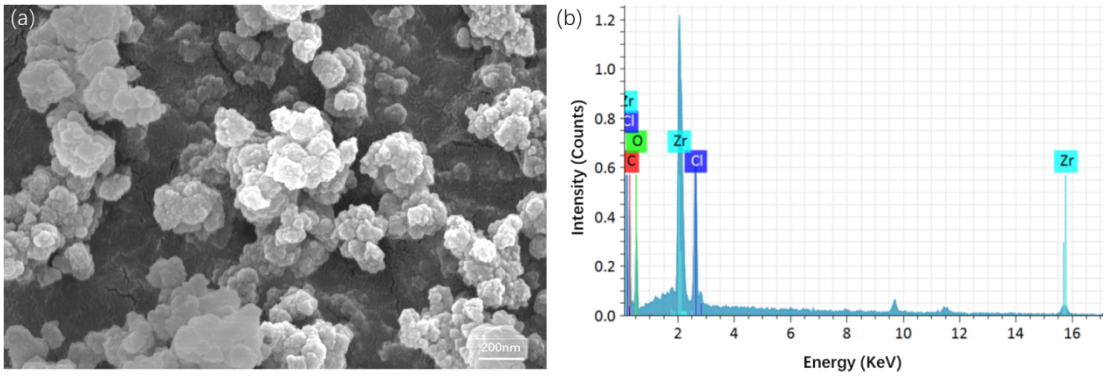

Fig. S1. (a) FE-SEM images of Zr-MOF. (b) The EDS peaks for Zr-MOF.

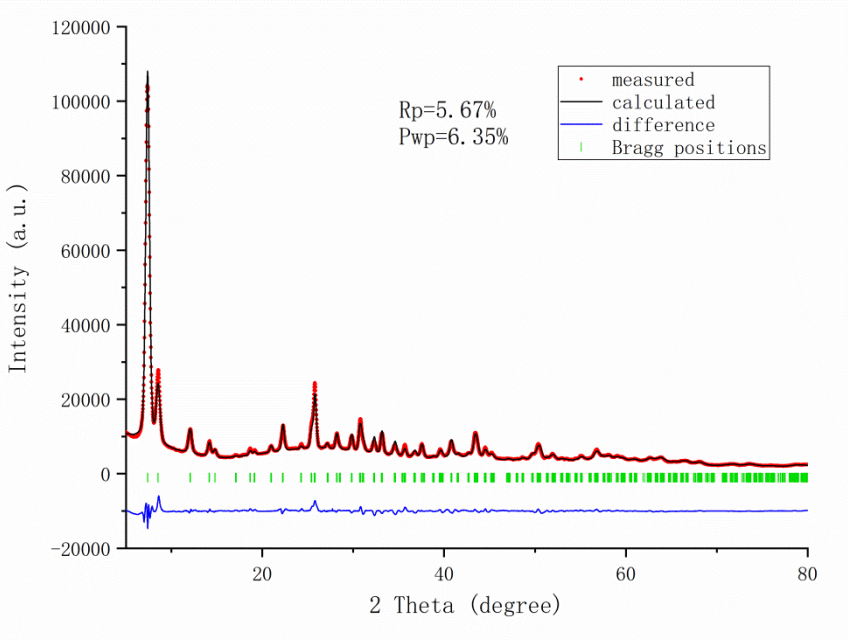

Fig. S2. Rietveld plot of Zr-MOF. Red: experimental points; black: calculated points; green: Bragg peaks; blue: difference pattern.

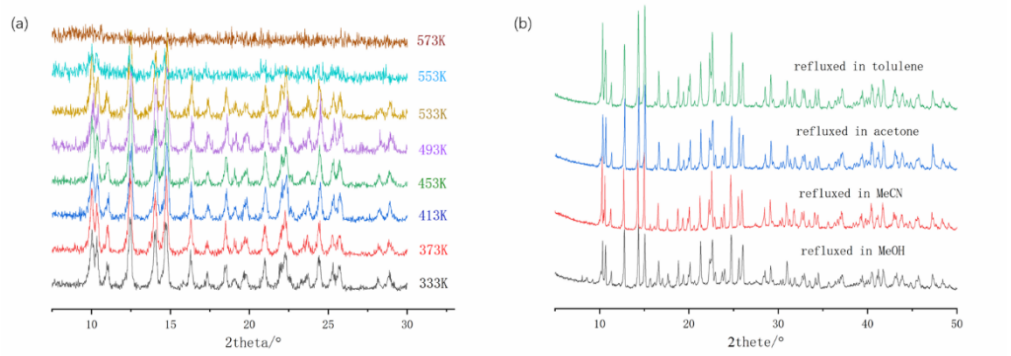

Fig. S3. (a) Temperature dependent XRD patterns of Gd-MOF from 333 K to 573 K. (b) PXRD patterns of the as-prepared Gd-MOF after refluxing in different solvents for 2 days.

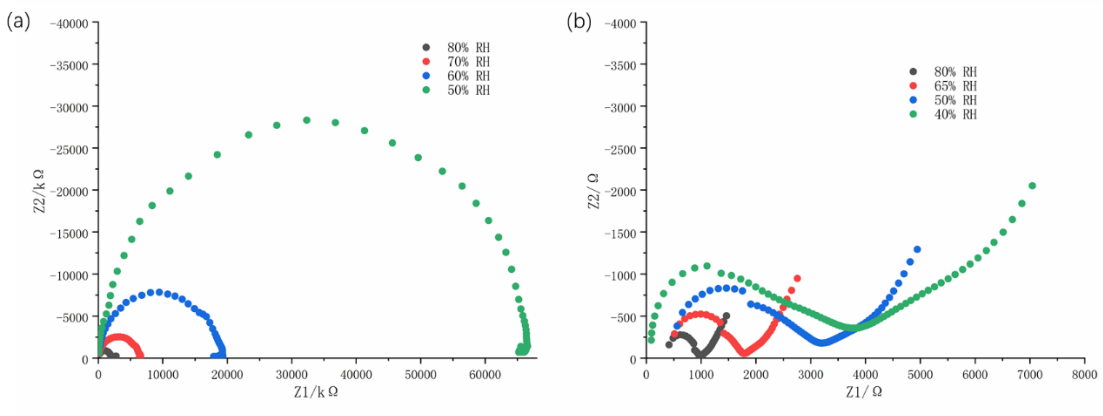

Fig. S4. (a) Nyquist plots of Gd-MOF at different relative humidity and 303 K. (b) Nyquist plots of Zr-MOF at different relative humidity and 303 K.

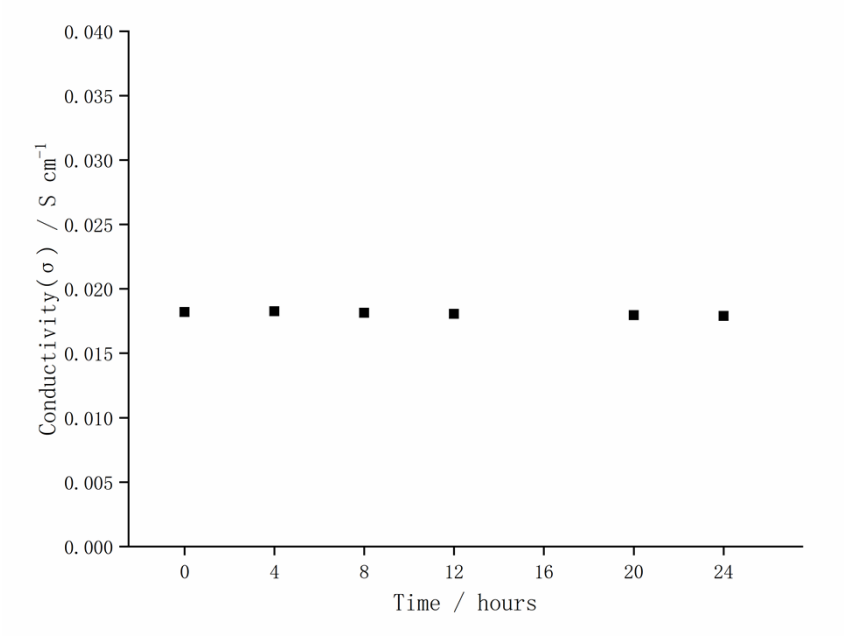

Fig. S5. Time-dependent proton conductivities of Zr-MOF at 353 K and 98% RH.